

CHAPTER 5

STABILITY AND CONVERGENCE ANALYSIS

The numerical stability plays a major role in checking the applicability of the method. The order and rate of convergence provide useful insights into the efficiency of the method while calculating numerical approximations. The stability analysis and convergence properties are discussed hereunder:

5.1 STABILITY ANALYSIS

Stability analysis is a study of how well a numerical solution behaves when applied to a linearized system. The numerical method is said to be stable if a small perturbation does not cause divergence from the solution (Mittal and Rohila, 2016). Further, an algorithm for solving a linear partial differential equation is said to be stable when the total variation of the numerical solution at a fixed time remains bounded as the step size goes to zero. Also, by analyzing the error and stability of a numerical technique, one can control the step size adaptively.

The stability of a time-dependent equation:

$$\frac{\partial C}{\partial t} = d(C), \quad (5.1)$$

where C is a function of both x and t and d is a spatial differential operator, is dependent upon the eigenvalues of the coefficient matrix of space discretization Eq. (5.1). Using the quintic Hermite collocation method, Eq. (5.1) is reduced into a set of ordinary differential equations in time:

$$\frac{dC}{dt} = [A]C + B. \quad (5.2)$$

where C is an unknown vector of the functional values at the interior grid points, B contains boundary values and nonhomogeneous part, and $[A]$ is the coefficient matrix obtained after discretization. The detail of the same has already been explained in section 4.9 of chapter 4:

$$\text{Linear model-1 and 2, } [A] = \frac{1}{Peh^2} (H_q^k)''(u_r) - \frac{1}{h} (H_q^k)'(u_r). \quad (5.3)$$

$$\text{Linear model-3, } [A] = \frac{1}{Peh^2} (H_q^k)''(u_r) - \frac{1}{h} (H_q^k)'(u_r) - \frac{\mu B_i}{Pe} (H_q^k)(u_r). \quad (5.4)$$

$$\text{Linear model - 4, } [A] = \frac{1}{R_d Peh^2} (H_q^k)''(u_r) - \frac{1}{R_d h} (H_q^k)'(u_r). \quad (5.5)$$

Nonlinear model-1 and 2,

$$[A] = \left[\frac{\left[1 + B_0 \left\{ (c_0 - c_s) H_q^k(u_r) + c_s \right\} \right]^2}{m C_F A_0 + \left[1 + B_0 \left\{ (c_0 - c_s) H_q^k(u_r) + c_s \right\} \right]^2} \right] \times \left[\frac{1}{P e h^2} (H_q^k)''(u_r) - \frac{1}{h} (H_q^k)'(u_r) \right] \quad (5.6)$$

$$\text{Nonlinear model -3, } [A] = \frac{1}{(1 + k\mu)} \left[\frac{1}{P e h^2} (H_q^k(u_r))'' - \frac{1}{h} (H_q^k)'(u_r) \right]. \quad (5.7)$$

where $q = 1, 2, \dots, 6, k = 1, 2, \dots, N$ and $r = 1, 2, 3, 4$.

It is well-known that the stability of Eq. (5.2) depends upon the stability of the numerical technique that is adopted to solve it. Any stable numerical technique for time discretization may not attain convergent solutions if the corresponding system of ordinary differential Eq. (5.2) is unstable. Mittal and Rohila (2016) explained in their study that the stability of Eq. (5.2) depends upon the Eigenvalues of the coefficient matrix A. Suppose λ_i to be the Eigenvalues of the coefficient matrix A.

According to Korkmaz and Dag (2011), when t approaches infinity, for the stable solution X one must have:

- (a) If all the Eigen values are real, $-2.78 < \Delta t \lambda_i < 0$;
- (b) If all the Eigenvalues have only complex components, $-2\sqrt{2} < \Delta t \lambda_i < 2\sqrt{2}$; and
- (c) If all the Eigen values are complex, $\Delta t \lambda_i$ should be in the region Figure 5.1.

The eigenvalues of linear model-1 and 2, linear model-3, and linear model-4 for $N = 51, \Delta t = 0.0001$ are plotted in Figures 5.2 to 5.4 respectively. Besides, the eigenvalues of the nonlinear model-1 and 2 and nonlinear model-3 are presented in Figures 5.5 and 5.6 respectively for the case when

$$c_0 = 0.57, A_0 = 0.0336, B_0 = 7.29, c_s = 0.005, \varepsilon = 0.957, \mu = \frac{1 - \varepsilon}{\varepsilon}, \\ C_F = 106.8, N = 51, \Delta t = 0.0001$$

From Figures 5.2 to 5.6, all the eigenvalues are complex and lie in the stability region. Hence, the system in Eq. (5.3) to Eq. (5.7) is stable.

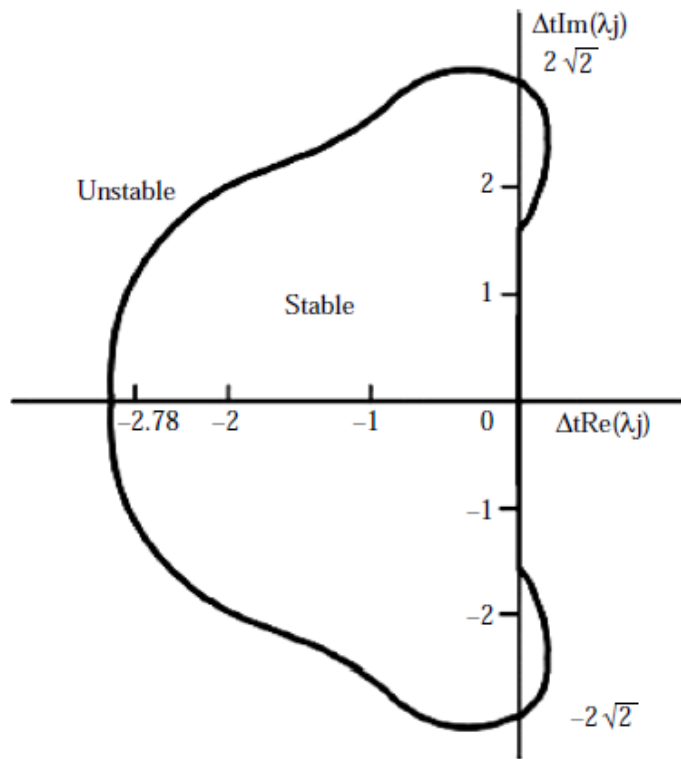


Figure 5.1 Stability region when eigenvalues are complex.

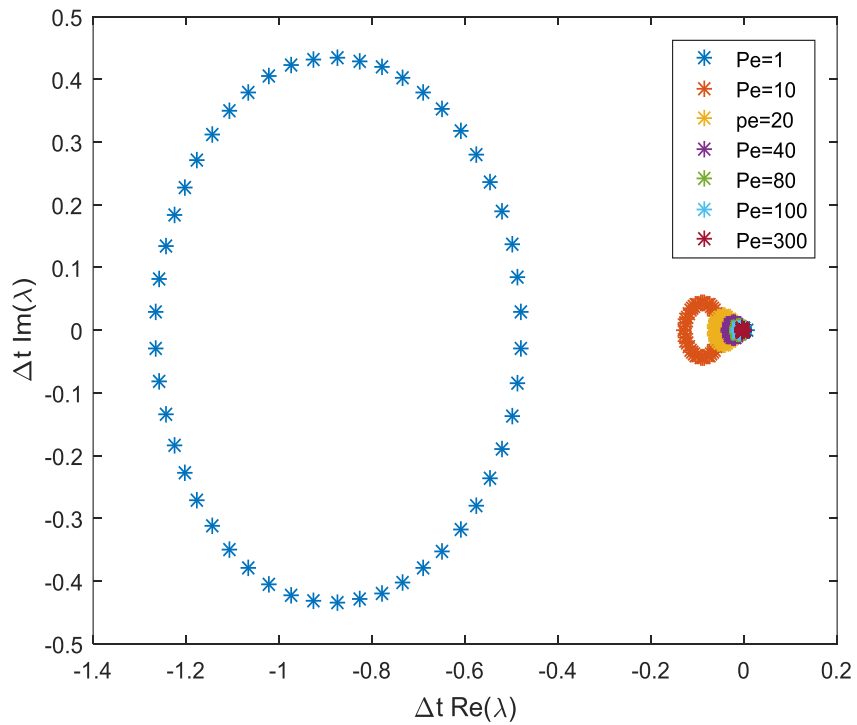


Figure 5.2 Eigenvalues of matrix A for linear model-1 and 2 with $N=51$, $\Delta t=0.0001$

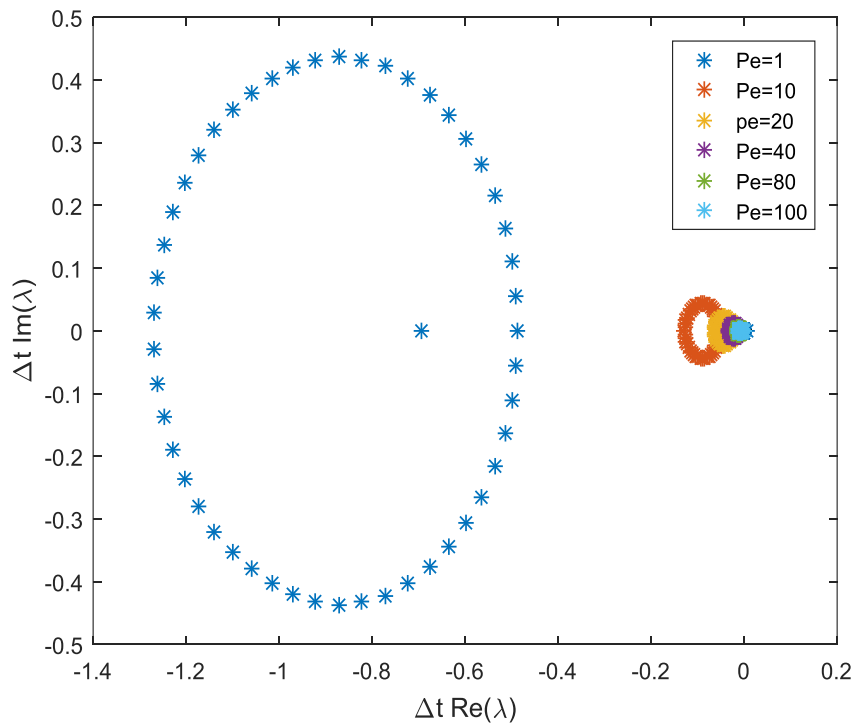


Figure 5.3 Eigenvalues of matrix A for linear model-3 with $N=51$, $\Delta t=0.0001$

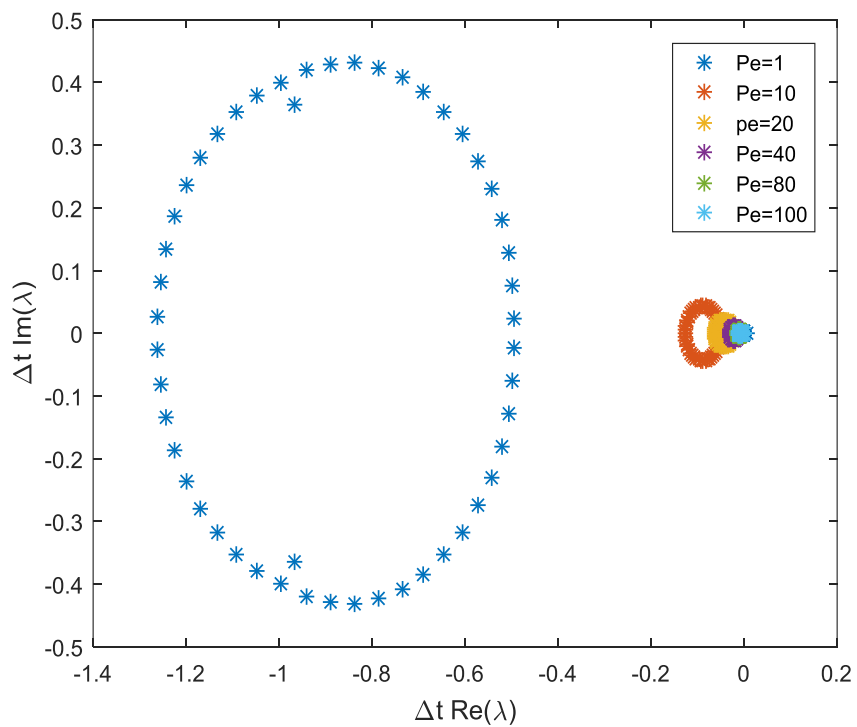


Figure 5.4 Eigenvalues of matrix A for linear model-4 with $N=51$, $\Delta t=0.0001$

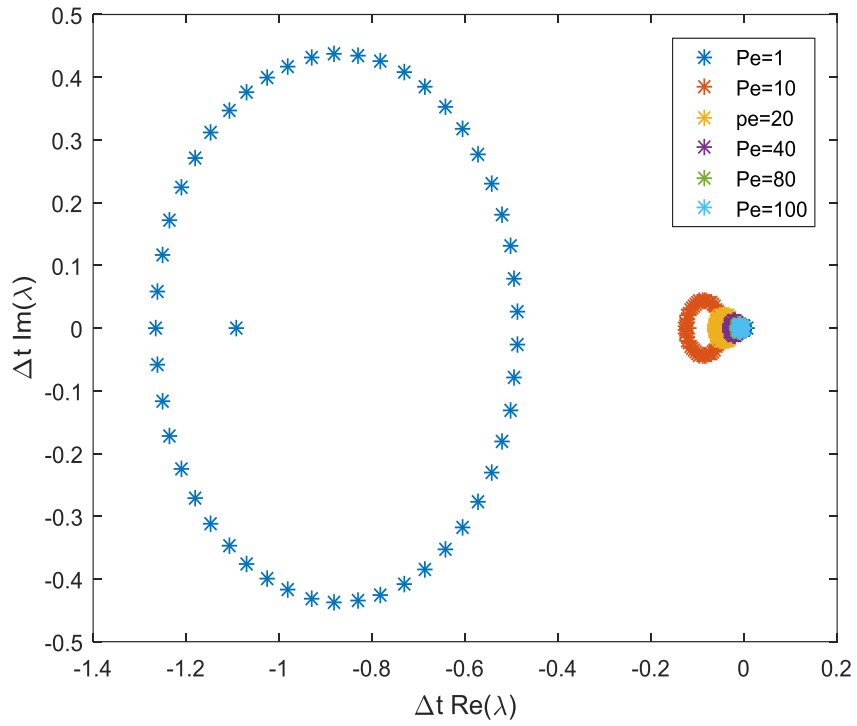


Figure 5.5 Eigenvalues of matrix A for nonlinear model-1 and 2 with $N=51$, $\Delta t=0.0001$

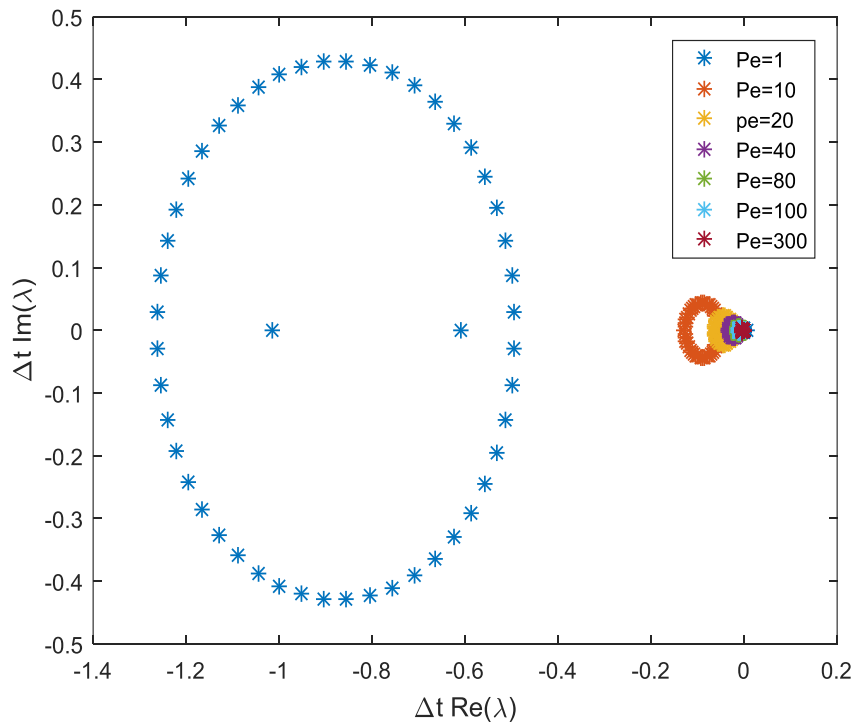


Figure 5.6 Eigenvalues of matrix A for nonlinear model-3 with $N=51$, $\Delta t=0.0001$

5.2 CONVERGENCE ANALYSIS

A numerical method is said to be convergent when the chosen step size diminishes or approaches zero, subsequently, the approximate numerical solution attained using the algorithm becomes the exact solution (Kumar and Kumari, 2019).

The mechanism of displacement washing of a packed bed of porous, compressible, and cylindrical particles, such as fibres, can be characterized mathematically with the help of the axial-dispersion model, viz:

$$\frac{\partial c}{\partial t} = \varepsilon \frac{\partial^2 c}{\partial z^2} - \alpha \frac{\partial c}{\partial z} - \beta c; (z, t) \in D, \quad (5.8)$$

It can be written as:

$$\mathfrak{S}_a c(z, t) \equiv \frac{\partial c}{\partial t} - \varepsilon \frac{\partial^2 c}{\partial z^2} + \alpha \frac{\partial c}{\partial z} + \beta c = g(z, t), \quad (5.9)$$

For boundary conditions:

$$k_1 c + k_2 \frac{\partial c}{\partial z} = 0 \quad \text{at} \quad z = 0 \quad \text{for} \quad t \in (0, T], \quad (5.10a)$$

$$k_3 c + k_4 \frac{\partial c}{\partial z} = 0 \quad \text{at} \quad z = 1 \quad \text{for} \quad t \in (0, T], \quad (5.10b)$$

and initial condition:

$$c(z, 0) = c_0(z). \quad (5.11)$$

where $D = \Omega \times (0, T] = (a, b) \times (0, T]$ and $c = c(z, t)$ are smooth functions $\forall z \in \Omega$.

Here $\varepsilon, \alpha, \beta, k_i$'s are real numbers.

5.2.1 Discretization Process

The trial function and discretization process are discussed in Chapter 3. Using this approximation technique, the discretized form obtained from equations Eq. (5.8), Eq. (5.10a), Eq. (5.10b), and Eq. (5.11) by using an approximate solution becomes:

$$\sum_{q=1}^6 \frac{da_{q+3(k-1)}}{dt} H_q^k(u_r) = \frac{\varepsilon}{h_k^2} \sum_{q=1}^6 a_{q+3(k-1)} \frac{d^2 H_q^k(u_r)}{du^2} - \frac{\alpha}{h_k} \sum_{q=1}^6 a_{q+3(k-1)} \frac{dH_q^k(u_r)}{du} - \beta \sum_{q=1}^6 a_{q+3(k-1)} H_q^k(u_r), \quad (5.12)$$

where $r = 2, 3, 4, 5$ (interior collocation points chosen as discussed above) and $k = 1, 2, \dots, N$ (number of elements).

$$k_1 \sum_{p=1}^6 a_{p+3(q-1)} H_p^q(1) + \frac{k_2}{h_k} \sum_{p=1}^6 a_{p+3(q-1)} \frac{dH_p^q(1)}{du} = 0; z=0 \quad , \quad (5.13a)$$

$$k_3 \sum_{p=1}^6 a_{p+3(q-1)} H_p^q(0) + \frac{k_4}{h_k} \sum_{p=1}^6 a_{p+3(q-1)} \frac{dH_p^q(0)}{du} = 0; z=1 \quad , \quad (5.13b)$$

$$\sum_{p=1}^6 a_{p+3(q-1)}(0) H_p^q(z) = c_0(z, 0) . \quad (5.14)$$

The residuals are set to zero at collocation points and the system of equations Eq. (5.12), Eq. (5.13a) and Eq. (5.13b) can be written as:

Figure 5.7 Matrix structure for the system of equations obtained using QHCM

The system of equations defined above can be expressed as:

$$Ab = d \quad , \quad (5.15)$$

where A is a matrix of the order $4N \times 4N$ containing collocation equations with boundary conditions at $z=0$ and $z=1$, b is the column matrix of collocation points of order $4N \times 1$ and d is the column matrix of the differential operator of order $4N \times 1$.

The obtained matrix structure is solved numerically by using the backward difference formula (BDF) with the algorithm developed for MATLAB ode 15s.

5.2.2 Time Discretization

In this process, the time domain is divided into the finite number of mesh points say (M) with a uniform step size Δt as given below:

$$\Omega_t = \{0 = t_0, t_1, t_2, \dots, t_M = T\} \quad \text{such that} \quad M\Delta t = T \quad \text{and} \quad \Delta t = |t_{M+1} - t_M|$$

Thereafter, using Euler implicit method in problem Eq. (5.8) can be discretized in the time domain as given below:

$$C(z, t_l) = C(z, t_{l+1}) - \Delta t \varepsilon \frac{\partial^2 C(z, t_{l+1})}{\partial z^2} + \Delta t \alpha \frac{\partial C(z, t_l)}{\partial z} + \Delta t \beta C; (z, t) \in \Omega_t, \quad (5.16)$$

Subject to the initial and boundary conditions

$$C(z, 0) = C_0(z),$$

From Eq. (5.10a) and Eq. (5.10b)

$$C(0, t_{l+1}) = \phi(0, t_{l+1}) \quad \text{where} \quad 0 \leq l+1 \leq M$$

$$C(1, t_{l+1}) = \phi(1, t_{l+1}) \quad \text{where} \quad 0 \leq l+1 \leq M$$

where $C(z, t_{l+1})$ is the numerical solution of Eq. (5.8) to Eq. (5.10b) at $(l+1)^{th}$ time level.

5.2.3 Convergence criteria

Lemma 1 [Kumar and Kumari (2019)]: Maximum Principal: Let the solution $c(z, t)$ of Eq. (5.8) be a smooth function with $c(0, t) \geq 0$ and $c(1, t) \geq 0$. Then $\Im c(z, t) \geq 0$ for all $(z, t) \in \Omega(0, 1)$ then we have $c(z, t) \geq 0$ for all $(z, t) \in \Omega(0, 1)$.

Lemma 2 [Kumar and Kadalbajoo (2011)]: Let $c(z, t)$ be the solution of Eq.(5.8) defined on $(z, t) \in \Omega(0, 1)$ then it is bounded by some K such that $c(z, t) \leq K$ for all $(z, t) \in \Omega(0, 1)$.

Proof: As Ross et al. (2008) have proved the result $c(z, t)$ defined $(z, t) \in \Omega(0, 1)$ given by:

$$|c(z, t) - c(0, t)| \leq K_t \quad \text{for } t \in (0, T]$$

$$\text{Then} \quad |c(z, t) - c(0, t)| \leq |c(z, t) - c(0, t)| \leq K_t$$

$$\text{Or} \quad |c(z, t)| \leq K \quad \text{when } |c(0, t)| + K_t \text{ is bounded by some constant } K.$$

Lemma 3: If Lemma 1 and 2 are hold , the bound of the derivative of the function $c(z, t)$ with respect to t is given as: $\left| \frac{\partial u}{\partial t} \right| \leq K$ for all $(z, t) \in \Omega(0, 1)$.

Proof: For the proof of the Lemma the readers can refer to available in Chakravarthy and Kumar (2019).

Lemma 4 [Chakravarthy and Kumar (2019)]: The bound for the i^{th} derivative of $c(z,t)$ with respect to z is given as:

$$\left| \frac{\partial^i u}{\partial t^i} \right| \leq K[1 + \varepsilon^{-i} \exp(-\alpha(1-z)/\varepsilon)] \text{ for all } (z,t) \in \Omega(0,1), i = 0,1$$

The local error measures the contribution of each time step to the global error of the time discretization given above.

Lemma 5: (Local error estimate) If $\left| \frac{\partial^i u}{\partial t^i} \right| \leq K$ for all $(z,t) \in \Omega(0,1)$,

Then the local error estimate in temporal direction is given as $\|e_{j+1}\| \leq K(\Delta t)^2$

where $e_{j+1} = C(z, t_{j+1}) - c(z, t_{j+1})$

Proof: From Eq. (5.16) we have

$$C(z, t_j) = C(z, t_{j+1}) - \Delta t \varepsilon \frac{\partial^2 C(z, t_{j+1})}{\partial z^2} + \Delta t \alpha \frac{\partial C(z, t_j)}{\partial z} + \Delta t \beta C; (z, t) \in \Omega_t \quad (5.17)$$

Also

$$c(z, t_j) = c(z, t_{j+1}) - \Delta t c_t(z, t_{j+1}) + \int_{t_j}^{t_{j+1}} (t_j - \varepsilon) c_{tt}(z, \xi) d\xi; (z, t) \in \Omega \quad (5.18)$$

Substituting the value of $c_t(z, t_j)$ from Eq. (5.17) in Eq. (5.18) one gets:

$$c(z, t_{j+1}) - c(z, t_j) = \Delta t [\varepsilon c_{zz}(z, t) - \alpha c_z(z, t) + \beta c] + O(\Delta t)^2; (z, t) \in \Omega_t \quad (5.19)$$

From Eq. (5.17) and Eq. (5.19) one gets:

$$\Delta t L(e_{j+1}) = O(\Delta t)^2; e_{j+1}(0) = e_{j+1}(1) = 0$$

Using the results of maximum principle given by Clavero et al. (2003), we obtain the desired result,

i.e., $\|e_{j+1}\| \leq K(\Delta t)^2$ where $e_{j+1} = c(z, t) - C(z, t)$

Theorem 1. (Global error estimate) Let E_n is the global error estimate in the temporal direction

then show that $\|E_n\|_{\infty} \leq K \Delta t$ where K is a positive constant.

Proof: As $E_{n+1} = \sum_{i=1}^n e_i$

$$\text{Also } \|E_{n+1}\|_{\infty} \leq \left\| \sum_{i=1}^n e_i \right\|_{\infty} \leq \|e_1\|_{\infty} + \|e_2\|_{\infty} + \dots + \|e_m\|_{\infty}$$

then using Lemma 5, we get

$$\|E_{n+1}\|_{\infty} \leq K_1(\Delta t)^2 + K_1(\Delta t)^2 + \dots + K_1(\Delta t)^2$$

$$\|E_{n+1}\|_{\infty} \leq K_1 n (\Delta t)^2 = K_1 (n \Delta t) (\Delta t) \leq K_1 T \Delta t, \text{ since } n \Delta t \leq T$$

$$\text{Implies } \|E_{n+1}\|_{\infty} \leq K \Delta t \text{ for } K_1 T = K$$

Therefore, the proposed numerical scheme is uniformly convergent of first order in temporal direction.

Theorem 2. Let $\tilde{c}(z)$ be the collocation approximation from space of quintic Hermite interpolation polynomial to the solution $c(z)$ of the differential equation such that $c(z) \in C^6[0,1]$. Then the uniform error estimate is given by:

$$\|c(z) - \tilde{c}(z)\|_{\infty} \leq K n^{-4} \ln^6(n) \text{ where } K \text{ is a positive constant}$$

Proof: Let $c_n(z)$ be the unique quintic Hermite interpolation for boundary value problem. The two cases arise when the mesh is divided into two regions $[0,1-t]$ and $[1-t,1]$.

For derivative of quintic Hermite polynomial Hall's error estimate (Hall, 1968) is used as given below:

$$\|D^j(c(z) - c_n(z))\|_{\infty} \leq \lambda_j h^{6-j} \|c^{(6)}\|_{\infty}; \quad 0 \leq j \leq 5$$

where,

$$\lambda_0 = \frac{1}{46,080}, \lambda_1 = \frac{\sqrt{5}}{30,000}, \lambda_2 = \frac{1}{1920}, \lambda_3 = \frac{1}{120}, \lambda_4 = \frac{1}{10}, \lambda_5 = \frac{1}{2}$$

$$\text{Now, } |\Im c(z_i) - \Im c_n(z_i)| \leq |\varepsilon| |c'(z_i) - c'_n(z_i)| + |\alpha| |c'(z_i) - c'_n(z_i)| + |\beta| |c(z_i) - c_n(z_i)|$$

It follows from Lemma 4

$$\begin{aligned} |\Im c(z_i) - \Im c_n(z_i)| &\leq (\varepsilon \lambda_2 h^4 + \alpha \lambda_1 h^5 + \beta \lambda_0 h^6) |c^{(6)}(z_i)| \\ |\Im c(z_i) - \Im c_n(z_i)| &\leq (\varepsilon \lambda_2 h^4 + \alpha \lambda_1 h^5 + \beta \lambda_0 h^6) (1 + \varepsilon^{-6} \exp(-\alpha(1-z_i)/\varepsilon)) \\ |\Im c(z_i) - \Im c_n(z_i)| &\leq \frac{h^4}{80} \left(\frac{\varepsilon}{24} + \frac{\sqrt{5} h \alpha}{375} + \frac{h^2 \beta}{576} \right) (1 + \varepsilon^{-6} \exp(-\alpha(1-z_i)/\varepsilon)) \end{aligned} \quad (5.20)$$

Case 1: Let $t=1/2$, In this case, the mesh is assumed to be uniform with spacing $h(1/n)$ and

$$(\varepsilon / \alpha) \ln(n) \geq \frac{1}{2}$$

Gives $\varepsilon^{-1} \leq K \ln(n)$ then from Eq. (5.20) one gets:

$$|\Im c(z_i) - \Im c_n(z_i)| \leq K n^{-4} \ln^6(n) \quad (5.21)$$

Case2: Let $t = (\varepsilon / \alpha) \ln(n)$, In this case, the mesh is piecewise uniform with space size $2(1-t) / n$ in the interval $[0,1-t]$ and $2t / n$ in $[1-t,1]$.

For $0 \leq i \leq \frac{n}{2}$ then by using Lemma 4 in the interval $[0, 1-t]$, one gets $|c^i(z)| \leq K$.

Also, from Eq. (5.20), one gets:

$$|\mathfrak{I}c(z_i) - \mathfrak{I}c_n(z_i)| \leq Kn^{-4} \quad (5.22)$$

If $\frac{n}{2} \leq i \leq n$, then we have $h = \frac{2t}{n} = \frac{\varepsilon \ln(n)}{\alpha n}$. Then from Eq. (5.20), one gets:

$$|\mathfrak{I}c(z_i) - \mathfrak{I}c_n(z_i)| \leq Kn^{-4} \ln^6(n) \quad (5.23)$$

Also, with the system of equations obtained, one gets:

$$A\tilde{b} = \tilde{d} \quad (5.24)$$

From Eq. (5.15) and Eq. (5.24)

$$A(b - \tilde{b}) = d - \tilde{d} \quad (5.25)$$

Also $\|d - \tilde{d}\|_\infty \leq Kn^{-4} \ln^6(n)$ and $\|A^{-1}\|_\infty \leq K$

Then from Eq. (5.25), one gets:

$$\|b - \tilde{b}\|_\infty \leq Kn^{-4} \ln^6(n)$$

And $c(z) - \tilde{c}(z) = \sum_{i=1}^6 [b(z) - \tilde{b}(z)]H_i(z)$

$$\|c(z) - \tilde{c}(z)\|_\infty \leq \max_{1 \leq i \leq 6} |c(z) - \tilde{c}(z)| \leq Kn^{-4} \ln^6(n)$$

Using triangular inequality, one gets:

$$\|c(z) - \tilde{c}(z)\|_\infty \leq Kn^{-4} \ln^6(n)$$

Hence the result is proved.

5.3 SUMMARY

In this chapter, the stability of the numerical technique is explained based on Eigenvalues. The Eigenvalues for linear and nonlinear models are complex and lie in the stability region. Besides this, the convergence analysis of the method is also discussed for uniform error estimates.